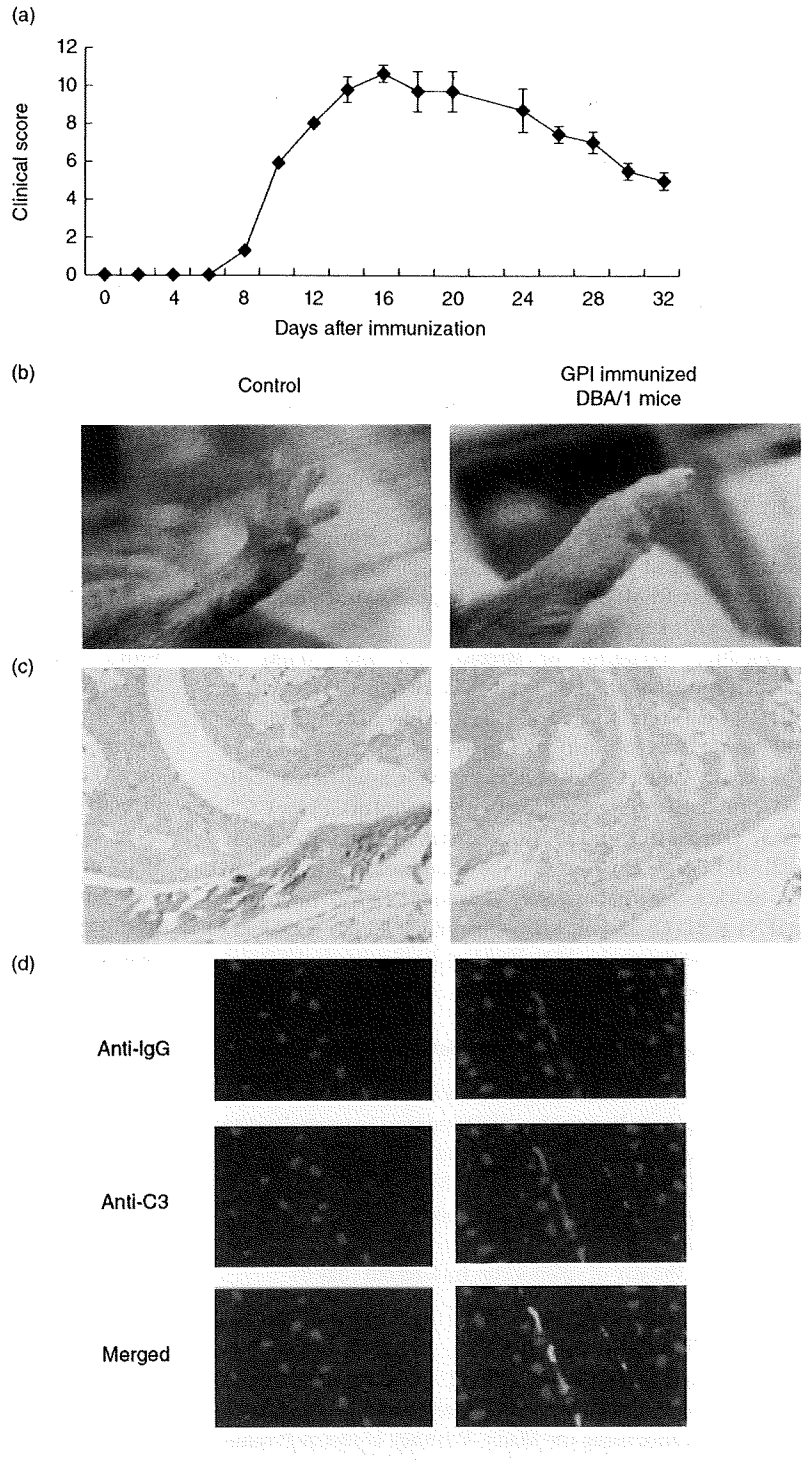

Fig. 1. Clinical and histological evaluation of glucose-6-phosphate isomerase (GPI)-induced arthritis in DBA/1 mice. Mean of clinical score (a) (±standard error of the mean, 10 mice) followed days after immunization. (b) Paw of control DBA/1 mouse treated with control antigens [gluthathione S-transferase (GST)] 300 μg (left). DBA/1 mice were immunized with rh-GPI 300 μg in Freund's complete adjuvant (CFA) (right). (c) Histological examination of ankle joints of the control (left) and GPI-induced arthritis on day 14 showing severe synovium proliferation (haematoxylin and eosin staining, right). (d) Anti-C3 (green) and anti-immunoglobulin (Ig)G (red) staining in joints of control (left) and arthritic DBA/1 mice (right). Nuclei were counterstained with 4,6-diamino-2-phenylindole (blue). C3 and IgG were co-localized on the surface of cartilage of ankle joints (right). Magnification of original photographs: ×40 (c) or ×600 (d); spl: splenocytes.

$CD19^+$ nor $CD4^+$ cell-depleted splenocytes induced arthritis in SCID mice (Fig. 4a), or produced anti-GPI antibodies (Fig. 4b), suggesting that both $CD19^+$ and $CD4^+$ cells play important roles in the induction of arthritis in SCID, and that production of anti-GPI antibodies may be indispensable for such induction.

Importance of B cells as producers of antibodies in arthritis of SCID mice

It has been reported previously that B cell-deficient mice are resistant to GPI-induced arthritis [9]. However, whether these cells act as autoantibody-producing cells as well as APCs

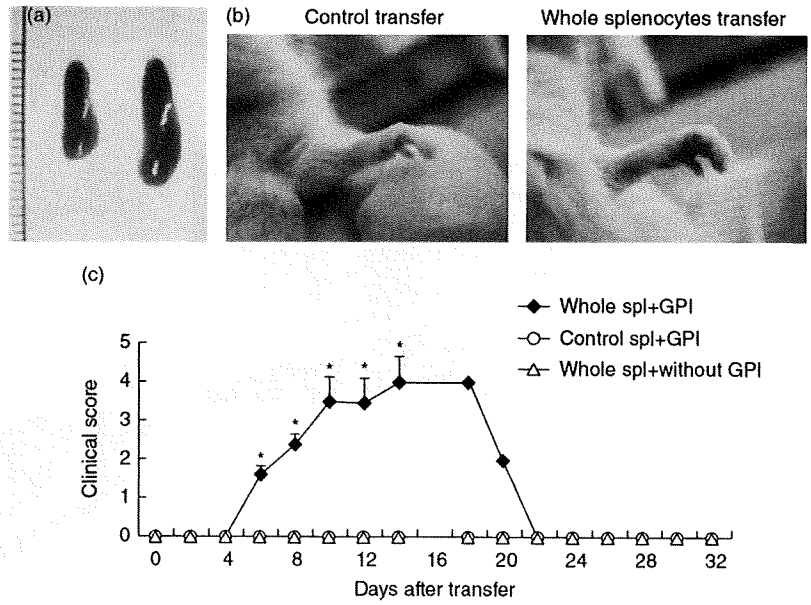

Fig. 2. Transfer of arthritis in SCID mice. Glucose-6-phosphate isomerase (GPI)-immunized DBA/1 mice were killed on day 14, and 1×10^7 splenocytes (spl) were isolated and transferred into SCID mice with 100 μg of GPI. (a) Spleen of control SCID mice (left) and SCID mice inoculated with splenocytes of arthritic DBA/1 mice 1×10^7 cells (right on day 14). (b) Feet of SCID mice inoculated with splenocytes from naive DBA/1 mice (left) and SCID mice inoculated with splenocytes from GPI-induced arthritic DBA/1 mice (right). (c) Clinical score and development of arthritis in SCID mice. Swelling of paws was observed on day 6 in SCID mice inoculated with whole splenocytes plus 100 μg of GPI (◆). Control mice were inoculated with 1×10^7 splenocytes only from immunized DBA/1 mice (△) or 1×10^7 splenocytes from control immunized DBA/1 mice plus 100 μg of GPI (○). Control mice did not develop arthritis. Data are mean ± standard error of the mean of five mice in each group. *$P < 0.05$ by Mann–Whitney *U*-test.

is unknown at present. To investigate the role of autoantibodies, we inoculated SCID mice with IgGs from arthritic DBA/1 mice. IgGs were purified from the sera of DBA/1 mice on day 14 after immunization. Injection of 3 mg IgG alone from arthriticDBA/1 mice did not result in overt arthritis in SCID mice, even if we added 100 μg of GPI (Fig. 5a). However, injection of IgG with $CD19^+$-depleted splenocytes and GPI resulted in the development of arthritis in SCID mice (Fig. 5a). To investigate further the arthritogenicity of anti-GPI antibodies, we used affinity purified anti-GPI antibodies from arthritic DBA/1 mice. Injection of 3 mg anti-GPI antibodies alone did not result in arthritis in SCID mice, even if we added 100 μg of GPI (Fig. 5b). However, with $CD19^+$-depleted splenocytes, even if we used 1 mg of affinity purified anti-GPI antibodies from GPI-induced mice instead of IgG, clear arthritis was developed in SCID mice (Fig. 5b). These findings suggest that $CD19^+$ cells play an important role as producers of antibody (especially anti-GPI antibodies) in arthritis of SCID mice; however, anti-GPI antibodies alone from GPI-induced arthritis do not have arthritogenecity.

Importance of TNF-α in the development of arthritis in SCID mice

To determine the humoral factors that were mediated by arthritis with splenocytes from GPI-induced arthritis plus GPI in SCID mice, we screened *in vitro* cytokine production from splenocytes plus GPI. We selected two proinflammatory cytokines in these experiments based on the preliminary results of cytometric beads array analysis, which revealed antigen-specific expression of TNF-α and IL-6 (data not shown); they have recently proved to be important in the induction of GPI-induced arthritis [12]. Indeed, the addition of GPI to the culture medium induced the production of large amounts of TNF-α and IL-6, while control antigen did not induce these cytokines (Fig. 6a). We also examined the production of these cytokines by $CD19^+$- and $CD4^+$-depleted cells. TNF-α and IL-6 levels were enhanced in the presence of $CD19^+$-depleted cells compared with $CD4^+$-depleted cells (Fig. 6a), and enriched slightly in $CD19^+$-depleted cells compared with whole splenocytes. To examine the role of IgG from DBA/1 arthritic mice, $CD19^+$-depleted splenocytes were stimulated with GPI and/or IgG *in vitro*. IgG triggered weak production of TNF-α and Fcγ blockade suppressed TNF-α production (Fig. 6b, $P < 0.05$). On the other hand, IL-6 production was regulated by neither IgG nor Fcγ blockade (Fig. 6b). To confirm the dependency of these inflammatory cytokines of arthritis in SCID mice, neutralizing mAbs were injected *in vivo* on the day of inoculation of splenocytes. Surprisingly, anti-TNF-α mAb protected arthritis completely in SCID mice, whereas anti-IL-6 mAb blocked arthritis partially (Fig. 6c). These findings suggest

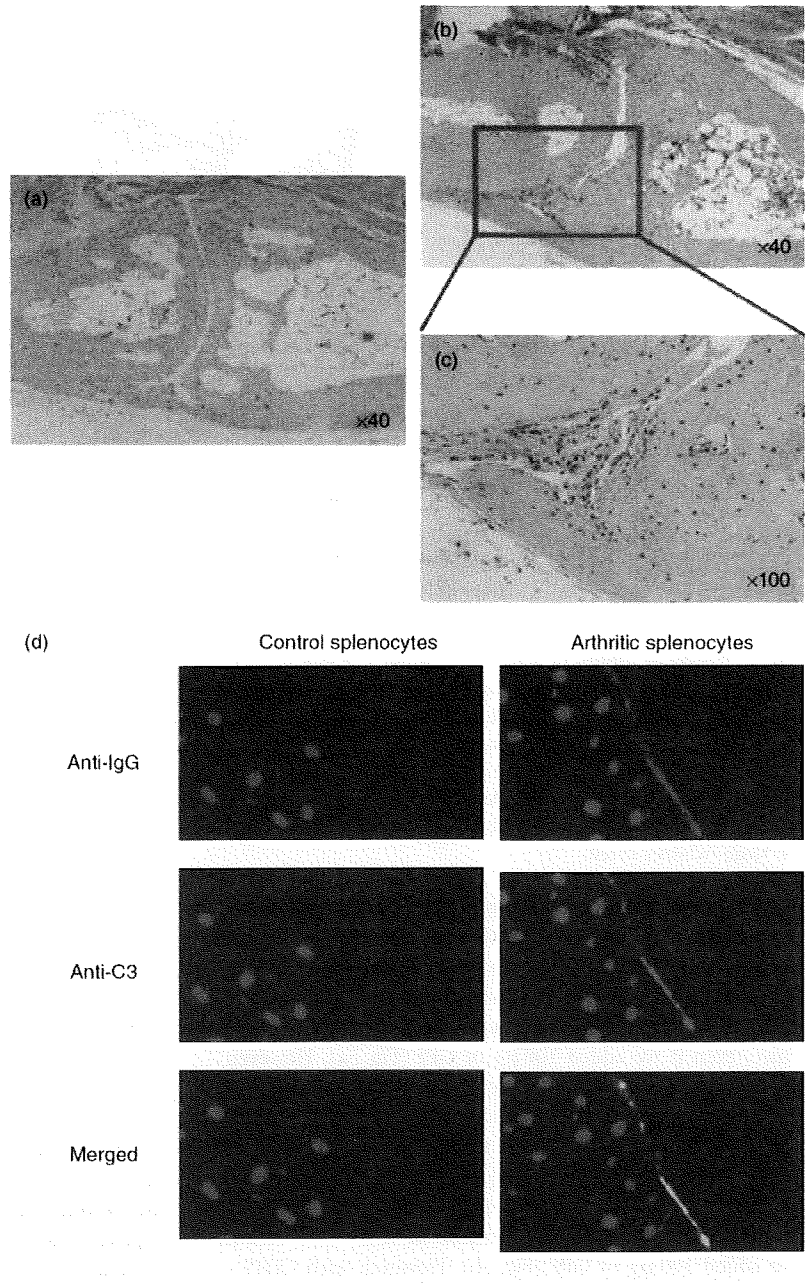

Fig. 3. Histological evaluation of joints of SCID mice. Joints of control mice inoculated splenocyte (spl) from naive DBA/1 mice with 100 μg of glucose-6-phosphate isomerase (GPI). (b,c) Synovial hyperplasia in a representative SCID mouse inoculated with splenocytes from arthritic DBA/1 mice. (d, right) Co-localization of immunoglobulin (Ig)G (red) and C3 (green) on the articular surface of SCID mice on day 14 after transfer by fluorescent staining. Nuclei were counterstained with 4,6-diamino-2-phenylindole (blue). Magnification of original photographs: ×40 (a), ×100 (b, c) or ×600 (d).

that TNF-α in particular (partially IL-6) induced by GPI may contribute to the development of arthritis, although IgG from arthritic mice contributed weakly to the production of TNF-α via Fcγ receptors.

CD11b$^+$ cells collaborating with CD4$^+$ T cells produce predominantly TNF-α

To analyse further the dominant cell populations that can produce TNF-α and IL-6, MACS-separated cells were co-cultured with GPI or GST (Fig. 7a,b). TNF-α was produced by several cell populations, driven mainly by CD11b$^+$ cells (Fig. 7a). It is possible that TNF-α production from CD11b cells was induced by the collaboration of activated T cells containing CD11b when cultured with GPI. On the other hand, IL-6 was produced predominantly by CD11c$^+$ cells (Fig. 7b). This cytokine production was enhanced by adding CD4$^+$ cells ($P < 0{\cdot}05$), thus CD4$^+$ T cells might also contribute for producing inflammatory cytokines.

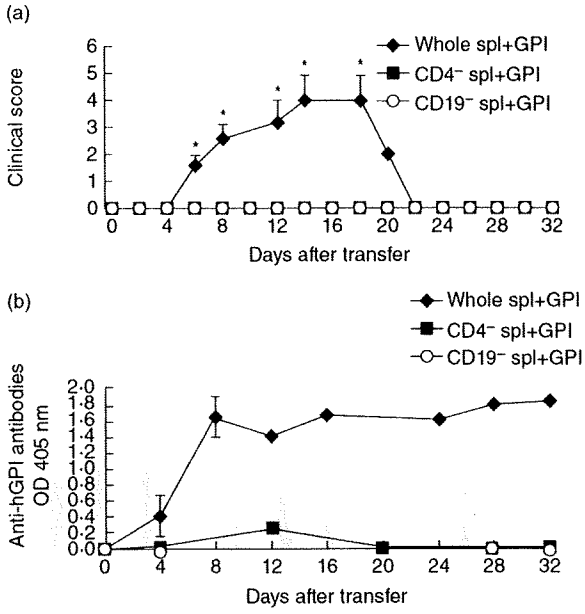

Fig. 4. Importance of anti-GPI antibodies in transfer of arthritis. CD19-depleted or CD4⁺-depleted splenocytes (spl) from arthritic DBA/1 mice obtained on day 14 after immunization were inoculated with glucose-6-phosphate isomerase (GPI) into SCID mice. (a) Mean clinical score. (b) Anti-GPI antibodies detected by enzyme-linked immunosorbent assay (ELISA) at 405 nm (b). (◆) SCID mice that received 1×10^7 of splenocytes from arthritic DBA/1 mice plus 100 μg GPI; (■) SCID mice recipients of 1×10^7 CD4⁺-depleted cells plus 100 μg GPI; (○) SCID mice recipients of 10^7 CD19-depleted cells plus 100 μg GPI. Data are mean ± standard error of the mean of five mice in each group. *$P < 0.05$ by Mann–Whitney U-test.

Exploring antigen-presenting function of B cells

Finally, to evaluate B cell function as APCs, MACS-separated CD4⁺ T cell and CD19⁺ cells were co-cultured with GPI. IFN-γ and IL-17 production were used to indicate the barometer of the antigen presentation function of B cells. Both IFN-γ and IL-17 were up-regulated clearly by adding CD19⁺ splenocytes ($P < 0.05$), indicating that CD19⁺ cell may function as APCs (Fig. 7c,d).

Discussion

Anti-GPI antibodies from K/BxN mice are well known as arthritogenic autoantibodies, and their effector mechanisms have been identified in several elegant studies [2–7]. Briefly, the key players involved in the development of arthritis after the transfer of anti-GPI antibodies included Fcγ receptor (particularly FcγRIII), alternative complement pathways such as factors B, C3, C5 and C5aR [3], subsets of Fcγ receptor or C5a receptor-bearing cells [4–6] and some inflammatory cytokines such as IL-1 and TNF-α [3]. In particular, a dominant pathological action driven by anti-GPI antibodies is a local association between GPI and anti-GPI on the articular surface, which leads to complement activation in the joints [7,13].

However, anti-GPI antibodies from GPI-induced arthritis did not induce overt arthritis in naive mice [8]. A previous report showed that B cell-deficient C3H.Q and B 10.Q mice were resistant to GPI-induced arthritis [9]. Moreover, FcγR-deficient mice were protected from GPI-induced arthritis, whereas mice deficient in inhibitory FcγRIIB developed severe arthritis [8]. These results show that B cells play an essential role in arthritis by producing autoantibodies that

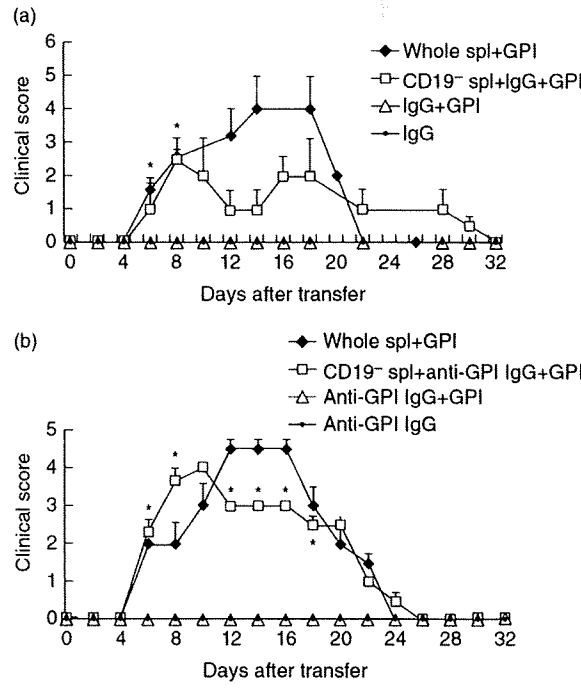

Fig. 5. Role of B cells in induction of arthritis in SCID mice. IgG from arthritic DBA/1 mice [alone or with glucose-6-phosphate isomerase (GPI)] or immunoglobulin (Ig)G plus CD19⁺-depleted cells were inoculated into SCID mice. Development of arthritis in SCID mice was monitored. (a) Mean clinical score is depicted. (◆) SCID mice that received 1×10^7 splenocytes (spl) plus 100 μg GPI; (□) SCID mice recipients of 1×10^7 CD19-depleted cells from arthritic DBA/1 mice with 3 mg of IgG plus 100 μg of GPI; (△) SCID mice recipients of 3 mg of IgG from arthritic DBA/1 mice plus 100 μg GPI; (•) SCID mice recipients of 3 mg of IgG from arthritic DBA/1 mice alone. (b) Affinity purified anti-GPI antibodies from arthritic DBA/1 mice (alone or with GPI), or anti-GPI antibodies plus CD19⁺-depleted cells were inoculated into SCID mice and monitored. (◆) SCID mice that received 1×10^7 spenocytes plus 100 μg GPI; (□) SCID mice recipients of 1×10^7 CD19-depleted cells from arthritic DBA/1 mice with 1 mg of anti-GPI antibodies plus 100 μg of GPI; (△) SCID mice recipients of 3 mg of anti-GPI antibodies from arthritic DBA/1 mice plus 100 μg GPI; (•) SCID mice recipients of 3 mg of anti-GPI antibodies from arthritic DBA/1 mice alone. Data are mean ± standard error of the mean of five mice in each group. *$P < 0.05$ by Mann–Whitney U-test.

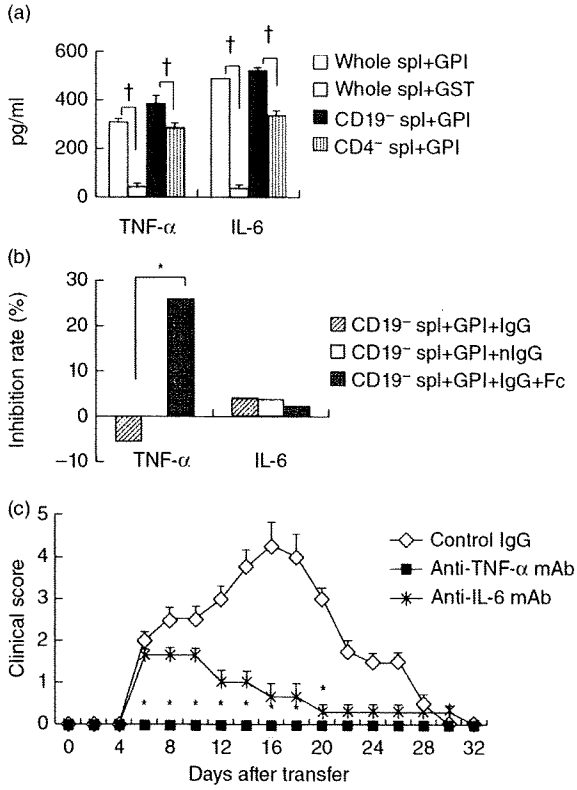

Fig. 6. *In vitro* cytokine production by splenocytes from arthritic DBA/1 mice and *in vivo* neutralization of inflammatory cytokines in SCID mice. Cytokine concentrations in supernatant of cultured splenocytes (spl) from arthritic DBA/1 mice were assessed by enzyme-linked immunosorbent assay. (a) Whole splenocytes or separated splenocytes (10^6 cell/ml) were cultured with 5 μg/ml of glucose-6-phosphate isomerase (GPI) or gluthathione S-transfererase (GST). (b) $CD19^+$-depleted splenocytes were cultured with GPI and immunoglobulin (Ig)G with/without FcγR blocker. IgG was purified from arthritic DBA/1 mice on day 14 after GPI immunization. Naive IgG (nIgG) was purified from naive DBA/1 mice. Inhibition rate was calculated to be divided by amount of productions from $CD19^+$-depleted splenocytes stimulated with GPI. Representative data of three independent experiments with three individual mice per experiment. (c) Neutralization of inflammatory cytokines was performed *in vivo* by monoclonal antibody (mAb), five mice in each group. SCID mice recipients of 1×10^7 splenocytes from arthritic DBA/1 mice plus 100 μg GPI and 100 μg of control IgG (◇), anti-tumour necrosis factor (TNF)-α mAb (■) or anti-interleukin (IL)-6 mAb (*). Data are mean ± standard error of the mean of five mice in each group. $^*P < 0.05$, $^\dagger P < 0.01$, by Mann–Whitney *U*-test.

result in FcγR activation in this model. In our immunohistological study, a clear complement activation by immune complex was observed in joints of mice with GPI-induced arthritis. This finding suggests that local immune complex (probably GPI–anti-GPI antibodies) activation in the joints also plays an important role in GPI-induced arthritis.

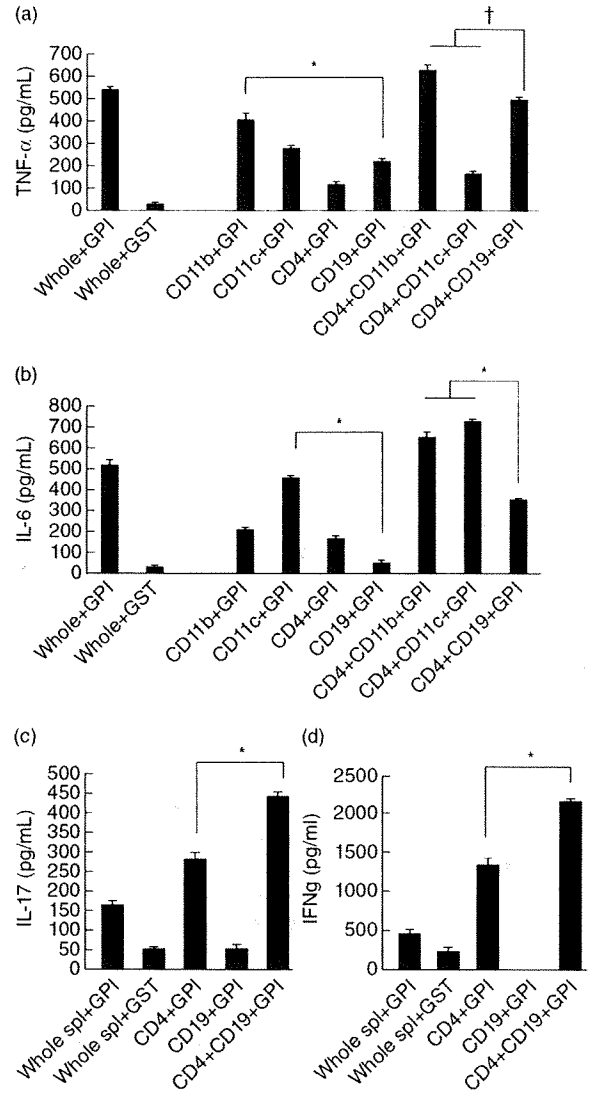

Fig. 7. Exploration of dominant cell population of inflammatory cytokines, and B cell functions as an antigen-presenting cells (APCs) *in vitro*. Whole splenocytes (spl) or independent magnetic affinity cell sorting (MACS) separated ($CD4^+$, $CD19^+$, $CD11b^+$ and $CD11c^+$ cells) splenocytes (total 1×10^6 cells/ml) were cultured with 5 μg/ml of glucose-6-phosphate isomerase (GPI) or gluthathione S-transfererase (GST). Inflammatory cytokines [tumour necrosis factor (TNF)-α (a) and interleukin (IL)-6 (b)] and T cell-secreted cytokines [IL-17 (c) and interferon (IFN)-γ (d)] were compared between $CD19^+$ cells and other APCs ($CD11b^+$ $CD11c^+$ cells). Cytokine concentrations in supernatant of cultured splenocytes from arthritic DBA/1 mice were assessed by enzyme-linked immunosorbent assay. The purity of cells was estimated by fluorescence activated cell sorter flow cytometry (> 90%). Data are mean ± standard error of the mean of three mice in each group. $^*P < 0.05$, $^\dagger P < 0.001$, by Mann–Whitney *U*-test.

To determine the role of B cells more precisely, we set up a transfer system using SCID mice. SCID mice inoculated with splenocytes from GPI-immunized DBA/1 mice together with GPI developed arthritis, and the immune complex activation was also noted on the articular surface of SCID mice. In GPI-induced arthritis, the expression of TNF-α mRNA in inflammatory joints and serum was increased on day 7 when detectable amounts of anti-GPI antibodies were produced (reference [12] and our unpublished data). B cell-depleted splenocytes from arthritic DBA/1 mice could not induce arthritis in SCID mice. On the other hand, SCID mice that received IgG (or anti-GPI antibodies) with B cell-depleted splenocytes from GPI-immunized DBA/1 mice developed arthritis, whereas SCID mice that received only IgG did not. These results suggest that B cells play a crucial role as antibody producers, followed by immune complex deposition on the articular surfaces in arthritis.

Our scenario is similar to adoptive transfer of collagen-induced arthritis (CIA) to SCID mice [14–16]. However, the GPI-induced arthritis in SCID mice occurred earlier (5–6 days) than CIA (14–16 days). The other difference between these two types of arthritis is that IgG from GPI-induced arthritis did not have arthritogenic capacity, whereas CIA IgG alone exhibit such capacity. Thus, anti-GPI antibodies produced by inoculated splenocytes play an important role in the induction of arthritis. However, these antibodies could not induce arthritis when injected alone, and thus we need to know about other humoral factors that trigger arthritis.

Our *in vitro* assay with splenocytes from GPI-induced arthritis plus GPI indicated that TNF-α and IL-6 may be crucial for the induction of arthritis. An earlier study from our laboratories identified the therapeutic efficacy of both anti-TNF-α mAb and anti-IL-6 mAb in GPI-induced arthritis [12]. Moreover, we clearly confirmed a protective effect of anti-TNF-α mAb in SCID-transferred arthritis. These results indicate that arthritis in SCID recipients may be enhanced mainly not only by anti-GPI antibodies, but also humoral factors such as TNF-α and IL-6. In particular, the development of arthritis was associated with the production of anti-GPI antibodies in SCID mice, thus autoantibodies might play a crucial role especially in the local joints, collaborating with inflammatory cytokines.

Concerning the other role of B cells, our *in vitro* assay suggests that B cells had a weak capacity of producing TNF-α, as well as antigen-presenting function with GPI culture. A recent paper reported that subsets of dendritic cells (DC) could express CD19 [17], thus it is possible that these cells comprise such functions of B cells. However, we tested *in vivo* experimentally with $CD19^+$-depleted cells, suggesting that the antoantibody produced indeed contributed to the development of arthritis.

What is the role of T cells in GPI-induced arthritis? Based on our experiments, splenocytes lacking $CD4^+$ cells failed to induce arthritis in SCID mice. The lack of anti-GPI antibodies in the serum of SCID recipients of the $CD4^+$ T cell-depleted cell population suggests that production of autoantibodies is $CD4^+$ T cell-dependent. Moreover, our *in vitro* assay identified $CD19^+$-depleted cells (probably comprising APCs plus T cells) as the main source of inflammatory cytokines that can trigger arthritis. TNF-α and IL-6 production was enhanced by adding $CD4^+$ cells, as confirmed by *in vitro* assay. In this regard, in GPI-induced arthritis, administration of anti-CD4 mAb on days 11 and 14 after immunization induced rapid remission of the arthritis [8]. We have reported previously that GPI-specific $CD4^+$ T cells were differentiated to T helper type 1 (Th1) and Th17 [18]. The administration of anti-IL-17 mAb on day 7 ameliorated arthritis significantly, whereas that administered on day 14 did not affect the disease. Moreover, *our vitro* assay using splenocytes on day 14 could detect tiny amounts of IL-17 with GPI ([17], and our unpublished data). These findings show that $CD4^+$ T cells (particularly Th17 cells) are necessary in the induction phase, and they function as supporters of production with autoantibodies and inflammatory cytokines in the effector phase of GPI-induced arthritis.

Are these scenarios relevant to human RA? High titres of anti-GPI antibodies are found in patients with severe forms of RA, but in only a few control individuals [10,19,20]. We reported recently that a *FCGR3A*-158V/F functional polymorphism was associated with RA in anti-GPI antibody-positive individuals, because 89% of healthy subjects positive for anti-GPI antibodies possessed homozygous low-affinity genotype *FCGR3A*-158F [21]. Moreover, among anti-GPI antibody-positive individuals, GPI-reactive $CD4^+$ T cells, especially Th1 cells, are detected specifically in peripheral blood mononucleocytes of patients with RA who share either human leucocyte antigen (HLA)-DRB1 *0405 or *0901 haplotypes [22]. These findings suggest that arthritis in anti-GPI antibody-positive individuals depends on several important factors, such as GPI-reactive T cells, HLA-DR*0405/*0901 and FcγRIII.

What of the role of anti-GPI antibodies in GPI-induced arthritis? The $H2^q$ haplotype confers severe form of arthritis [9]. High titres of anti-GPI antibodies were also found in arthritis-resistant C57BL/6($H2^b$) mice, although their T cells had weak GPI responses ([8], and our observations) compared with arthritis-susceptible DBA/1 mice. In addition, $Fc\gamma R^{-/-}$ mice are protected from GPI-induced arthritis, whereas $Fc\gamma RIIB^{-/-}$ mice developed pronounced arthritis [8]. These findings indicate that anti-GPI antibodies do not induce arthritis *per se*; it is probable that unique activation of major histocompatibility complex class II and antigen-specific T cells might be indispensable. In this regard, GPI-induced arthritis appears to be akin to human RA.

In conclusion, we identified that B cells play a crucial role in GPI-induced arthritis as autoantibody producers. This finding might explain how autoantibodies orchestrate the induction of arthritis with inflammatory cytokines such as TNF-α in patients with RA.

Acknowledgements

We thank Miss Yuri Ogamino for excellent technical assistance. This work was supported in part by a grant from the Japanese Ministry of Science and Culture (I. M., T. S.).

References

1 Kannann KR, Ortmann A, Kimpel D. Animal models of rheumatoid arthritis and their relevance to human disease. Pathophysiology 2005; **12**:167–81.

2 Matsumoto I, Staub A, Benoist C, Mathis D. Arthritis provoked by linked T and B cell recognition of glycolytic enzyme. Science 1999; **286**:1732–5.

3 Ji H, Ohmura K, Mahmood U *et al.* Arthritis critically dependent on innate immune system players. Immunity 2001; **16**:157–68.

4 Binstadt BA, Patel PR, Alencar H *et al.* Particularities of the vasculature can promote the organ specificity of autoimmune attack. Nat Immunol 2006; **7**:284–92.

5 Wipke BT, Allen PM. Essential role of neutrophils in the initiation and progression of a murine model of rheumatoid arthritis. J Immunol 2001; **167**:1601–8.

6 Lee DM, Friend DS, Gurish MF *et al.* Mast cells: a cellular link between autoantibodies and inflammatory arthritis. Science 2002; **297**:1689–92.

7 Matsumoto I, Maccioni M, Lee DM *et al.* How antibodies to ubiquitous cytoplasmic enzyme may provoke joint-specific autoimmune disease. Nat Immunol 2002; **3**:360–5.

8 Schubert D, Maier B, Moraweitz L *et al.* Immunization with glucose-6-phosphate isomerase induced T cell-dependent peripheral polyarthritis in genetically unaltered mice. J Immunol 2004; **172**:4503–9.

9 Bockermann R, Schubert D, Kamradt T *et al.* Induction of a B-cell-dependent chronic arthritis with glucose-6-phosphate isomerase. Arthritis Res Ther 2005; **7**:1316–24.

10 Matsumoto I, Lee DM, Goldbach-Mansky R *et al.* Low prevalence of antibodies to glucose-6-phosphate isomerase in patients with rheumatoid arthritis and a spectrum of other chronic autoimmune disorders. Arthritis Rheum 2003; **48**:944–54.

11 Mori S, Sawai T, Teshima T, Kyogoku M. A new decalcifying technique for immunohistochemical studies of calcified tissue, especially applicable to cell surface marker demonstration. J Histochem Cytochem 1988; **36**:111–4.

12 Matsumoto I, Zhang H, Yasukochi T *et al.* Therapeutic effects of antibodies to TNFalpha and IL-6 and CTLA-4 Ig in mice with glucose-6-phosphate isomerase-induced arthritis. Arthritis Res Ther 2008; **10**:R66.

13 Wipke BT, Wang Z, Nagengast W *et al.* Staging the initiation of autoantibody-induced arthritis: a critical role for immune complex. J Immunol 2004; **172**:7694–702.

14 Williams RO, Plater-Zyberk C, Williams DG, Maini RN. Successful transfer of collagen-induced arthritis to severe combined immunodeficient (SCID) mice. Clin Exp Immunol 1992; **88**:455–60.

15 Kadowaki KM, Matsuno H, Tsuji H, Tunru I. $CD4^+$ T cells from collagen-induced arthritic mice are essential to transfer arthritis into severe combined immunodeficient mice. Clin Exp Immunol 1994; **97**:212–8.

16 Taylor PC, Pleter-Zyverk C, Maini RN. The role of the B cells in the adoptive transfer of collagen-induced arthritis form DBA/1 ($H\text{-}2^q$) to SCID (H-2d) mice. Eur J Immunol 1995; **25**:763–9.

17 Baban B, Hansen AM, Chandler PR *et al.* A minor population of splenic dendritic cells expressing CD19 mediates IDO-dependent T cell suppression via type I IFN signaling following B7 ligation. Int Immunol 2005; **17**:909–19.

18 Iwanami K, Matsumoto I, Tanaka-Watanabe Y *et al.* Crucial role of IL-6/IL-17 cytokine axis in the induction of arthritis by glucose-6-phosphate isomerase. Arthritis Rheum 2008; **58**:754–63.

19 van Gaalen FA, Toes RE, Ditzel HJ *et al.* Association of autoantibodies to glucose-6-phosphate isomerase with extraarticular complications in rheumatoid arthritis. Arthritis Rheum 2004; **50**:395–9.

20 Kassahn D, Kolb C, Solomon S *et al.* Few human autoimmune sera detect GPI. Nat Immunol 2002; **3**:411–2.

21 Matsumoto I, Zhang H, Muraki Y *et al.* A functional variant of Fcg receptor IIIA is associated with rheumatoid arthritis in anti-glucose-6-phosphate isomerase antibodies-positive individuals. Arthritis Res Ther 2005; **7**:1183–8.

22 Kori Y, Matsumoto I, Zhang H *et al.* Characterization of Th1/Th2 type, glucose-6-phosphate isomerase reactive T cells in the generation of rheumatoid arthritis. Ann Rheum Dis 2006; **65**:968–9.

Mod Rheumatol (2009) 19:358–365
DOI 10.1007/s10165-009-0172-2

ORIGINAL ARTICLE

A new low-field extremity magnetic resonance imaging and proposed compact MRI score: evaluation of anti-tumor necrosis factor biologics on rheumatoid arthritis

Takeshi Suzuki · Satoshi Ito · Shinya Handa · Katsumi Kose · Yoshikazu Okamoto · Manabu Minami · Taichi Hayashi · Daisuke Goto · Isao Matsumoto · Takayuki Sumida

Received: 5 December 2008 / Accepted: 23 March 2009 / Published online: 16 April 2009

Abstract Magnetic resonance imaging (MRI) is a useful tool for evaluating disease activity and therapeutic efficacy in rheumatoid arthritis (RA). However, conventional whole-body MRI is inconvenient on several levels. We have therefore developed a new low-field extremity MRI (compact MRI, cMRI) and examined its clinical utility. Thirteen RA patients treated with anti-tumor necrosis factor (TNF) biologics were included in the study. The MRI was performed twice using a 0.21-T extremity MRI system. The MRI images were scored using our proposed cMRI scoring system, which we devised with reference to the Outcome Measures in Rheumatology Clinical Trials RA MRI score (OMERACT RAMRIS). In our cMRI scoring system, synovitis, bone edema, and bone erosion are separately graded on a scale from 0 to 3 by imaging over the whole hand, including the proximal interphalangeal joint. The total cMRI score (cMRIS) is then obtained by calculating the total bone erosion score × 1.5 + total bone edema score × 1.25 + total synovitis score. In this study, one patient showed a progression of bone destruction even under low clinical activity, as assessed by the disease activity score on 28 joints (DAS28); however, another patient's cMRIS decreased concurrently with the decrease in DAS28, with the positive correlation observed between ΔDAS28 and ΔcMRIS ($R = 0.055$, $P < 0.05$). We conclude that cMRI and cMRIS are useful for assessing total disease activity and as a method linking MRI image evaluation to clinical evaluation.

Keywords Anti-TNF biologics · Bone edema · Bone erosion · Low-field extremity MRI · MRI scoring system · Rheumatoid arthritis

T. Suzuki · S. Ito · T. Hayashi · D. Goto · I. Matsumoto · T. Sumida
Division of Clinical Immunology, Doctoral Program in Clinical Sciences, Graduate School of Comprehensive Human Sciences, University of Tsukuba, Tsukuba, Ibaraki, Japan

S. Handa · K. Kose
Institute of Applied Physics, University of Tsukuba, Tsukuba, Ibaraki, Japan

Y. Okamoto · M. Minami
Department of Radiology, Institute of Clinical Medicine, University of Tsukuba, Tsukuba, Ibaraki, Japan

T. Sumida (✉)
Division of Clinical Immunology, Doctoral Program in Clinical Sciences, Graduate School of Comprehensive Human Science, University of Tsukuba, 1-1-1 Tennodai, Tsukuba, Ibaraki 305-8575, Japan
e-mail: tsumida@md.tsukuba.ac.jp

Introduction

Rheumatoid arthritis (RA) is a systemic inflammatory autoimmune disease that predominantly affects the synovial membranes of joints. Persistent inflammation or synovitis leads to pannus formation and, ultimately, bone destruction. A therapeutic window [1] does exist early in the RA course; therefore, the development of better methods for the early diagnosis and treatment of RA is one of the prime objectives of rheumatologists. Conventional radiography is currently the major tool for diagnosing RA and monitoring the progression of joint destruction. However, because this technique visualizes only late signs of preceding disease activity, other diagnostic tools, such as magnetic resonance imaging (MRI), have been the focus of increasing attention in recent years. Magnetic resonance

imaging is three- to sevenfold more sensitive than conventional radiography in terms of detecting joint erosion in early-stage RA [2, 3]. It can also detect synovitis, bone edema, and tenosynovitis that is not visible on conventional radiographic scans [4, 5]. Synovitis is among the earliest abnormalities observed in RA and is, in many cases, already apparent before a patient complains of joint pain or shows elevated serum C-reactive protein (CRP). The degree of bone marrow edema in metacarpalphalangeal (MCP) and wrist joints has recently been reported to be a more important predicator of radiographic progression in early RA than the degree of synovitis, erosion, or disease activity score based on 28 joints (DAS28) [6]. Evaluating bone edema by MRI may therefore assist clinicians in determining whether a patient should receive early and aggressive treatment to avoid subsequent joint damage.

While MRI may provide significant information about the course of RA not obtainable by conventional radiography, conventional whole-body, high-field MRI is more expensive in terms of both startup costs and maintenance fees, and it is not always convenient. In addition, claustrophobic patients and those suffering severe joint pain are sometimes unable to complete the examination. Low-field extremity MRI was recently developed to address these limitations; it is now commercially available and has been used clinically to evaluate RA. Low-field extremity MRI offers adequate performance at a lower cost and with greater comfort and convenience to the patient than conventional MRI [7, 8]. One strong disadvantage of this tool, however, is that the field of view (FOV) is too small to assess hand and wrist joints in one examination or in one sequence—and RA usually affects the wrist to proximal interphalangeal (PIP) joints. This is a major limiting factor in the success of low-field MRI for diagnosing of RA or assessing disease activity.

We have recently developed a new low-field extremity MRI system with a FOV large enough to simultaneously assess the entire wrist to PIP joint area. In the study reported here, we examined the clinical value of our low-field MRI system for assessing disease activity in RA patients treated with anti-tumor necrosis factor (TNF) biologics using the original scoring system.

Patients and methods

Patients and clinical assessments

Thirteen RA outpatients were enrolled in the study (two men and 11 women). The mean disease duration at evaluation was 6.2 years. Seven patients were treated with infliximab (IFX) and six with etanercept (ETN). Clinical disease activity was determined using the DAS28–CRP. Eleven patients had moderate or high disease activity before receiving anti-TNF biologics; the remaining patients had low clinical disease activity but showed bone destruction in the wrists, which had worsened significantly within the past year, as assessed by radiography. The IFX group also received an average methotrexate dose of 8 mg/week, with six patients also treated with prednisolone (average dose 7.1 mg/day). In the ETN group, four patients also received methotrexate (average dose 5 mg/week), and all six patients were taking prednisolone (average dose 5.3 mg/day). Table 1 presents additional sociodemographic data on these patients. All patients underwent two MRI assessments; the first was carried out at the time of starting the biologics (IFX group patients 5–7; ETN group patient 6) or within 7 and 9 months from the initial infusion of IFX and ETN (IFX group patients 1–4 and ETN group patients 1–5), respectively, and the second MRI assessment was within 8–16 months and 5–23 months from the first infusion for the respective groups.

New low-field extremity MRI system and MRI protocols

The new system is called compact MRI (cMRI). It comprises a permanent magnet, a gradient coil set, and an MRI console, generating a magnetic field strength of 0.21 T. The system occupies a total installation space of 4 m^2. The magnet is placed in an electromagnetic shield room [1.6 (W) × 2.0 (H) × 2.4 (D)] to prevent external noise. Patients sit in front of the magnet and insert one hand into the radio frequency (RF) coil for MR imaging. Coronal three-dimensional (3-D) gradient recalled echo T1-weighted images [repetition time (TR)/echo time (TE) = 50/9 ms] were obtained with an image matrix size at 512 × 384 × 32, FOV of 20.48 × 15.36 × 6.4 cm, and a scan time of 7 min and 5 s. Coronal 3D fast short tau inversion recovery (STIR) images [TR/TE/inversion time (TI) = 1000/60/100 ms] were also obtained with an image matrix size of 256 × 256 × 8, FOV at 20.48 × 20.48 × 6.4 cm, and a scan time of 8 min and 30 s. Both hands were scanned in all patients. The total examination time, including patient positioning, required about 40 min.

Image evaluation and proposed compact MRI score

Magnetic resonance imaging findings are currently scored using the RA MRI scoring system (RAMRIS) as reported in the Outcome Measures in Rheumatology Clinical Trials (OMERACT) [9]. However, the RAMRIS system requires a two-dimensional (2-D) analysis, and our cMRI system can analyze only the coronary section; consequently, RAMRIS cannot be used in our system. Our modified MRI system can visualize joints from the wrist to PIP in only one image. We

Table 1 Patients' demographics

Patient	Age (years)	Sex	Disease duration (years)	Stage[a]	Class[a]	MTX (mg/week)	PSL (mg/day)	Other DMARDs
Infliximab group								
1	51	F	1	2	2	10	10	SASP
2	58	F	5	2	1	8	0	BC
3	31	F	6	3	3	8	4	
4	48	F	11	4	3	6	15	
5	55	F	14	3	3	8	12.5	
6	30	F	2	1	1	8	4	
7	39	F	4	3	2	8	4	
Average	44.6		6.1	2	2	8	7.1	
Etanercept group								
1	68	M	3	4	2	8	5	
2	18	F	2	2	1	12	6	
3	54	M	3	3	2	4	6	SASP
4	59	F	12	4	3	0	10	SASP, ACT
5	42	F	10	2	1	0	4	
6	33	F	8	4	2	6	1	
Average	45.7		6	3	2	5	5.3	

F Female, *M* male, *MTX* methotrexate, *PSL* prednisolone, *DMARDs* disease-modifying antirheumatic drugs, *SASP* salazosulfapyridine, *ACT* Actarit, *BC* bucillamine

[a] Stage was determined according to the Steinblocker's classification, and class was determined according to the Hochberg's classification

therefore evaluated the images using our original scoring system, to obtain a compact MRI score (cMRIS) referenced to RAMRIS. The cMRIS scores the degree of bone erosion, bone marrow edema, and synovitis in both hands. In this study, the MRI images were reviewed by one radiologist, who is a Board-certified radiologist (by the authority of the Japan Radiological Society), and by more than two rheumatologists. All patients' information was blinded. Bone erosion and edema were defined using the OMERACT MRI joint pathology definition [10]. Bone erosion was defined by the presence of a sharply marginated bone region that was imaged as a loss of normal signal intensity of cortical bone and a loss of normal high signal characteristics, visible in two planes, with a cortical break seen in at least one plane on the T1-weighted image. Bone edema was defined a lesion within the trabecular bone, with ill-defined margins and signal characteristics consistent with increased water content that was imaged as high-intense signal on STIR and a low-intense signal on the T1-weighted image. Since we did not use gadolinium enhancement, synovitis was defined a high signal intensity on STIR that seemed anatomically to be the synovial area. The RAMRIS rates bone erosion from 0 to 10 by volume, while our scoring system rates bone erosion on a scale from 0 to 3 by volume. Bone edema and synovitis were scored on the same scale as RAMRIS. The PIP joints were scored by the same method used for the evaluating the MCP joints. This study evaluated 23 bones and 11 joints (Fig. 1). Bone erosion and edema were estimated in one to five MCP joints and one to five carpometacarpal (CM) joints, in two to five proximal and distal PIP joints, and in all wrist bones, except for the pisiforme, distal radius, and head of ulna. In the PIP and MCP joints, we evaluated each proximal and each distal side separately. and the score of the worse side was counted. Thus, the total estimation site of bone erosion and edema was 32. Synovitis, which was also scored on a scale from 0 to 3, was evaluated in two to five PIP joints, one to five MCP joints, and in the intercarpal and distal radioulnar joints. However, the intercarpal joint synovitis score was doubled because of its large volume. The overall score was calculated as follows: total synovitis score + 1.25 × total bone edema score + 1.5 × total bone erosion score [maximum total bone erosion score 207 (3 × 23 × 1.5 × 2), maximum total bone edema score 172.5 (3 × 23 × 1.25 × 2), maximum total synovitis score 72 {(3 × 10 + 3 × 1 × 2) × 2}; maximum cMRIS 451.5]. Further details of the scoring system are provided in Table 2.

Statistical analysis

The correlation between the changes in cMRIS (ΔcMRIS) and the DAS28–CRP (ΔDAS28) values was evaluated by Pearson's correlation coefficient test. A value of $P < 0.05$ was considered to be significant.

Results

Evaluation of DAS28-CRP

The DAS28–CRP was evaluated prior to the biologics treatment and at the time of first and second MRI

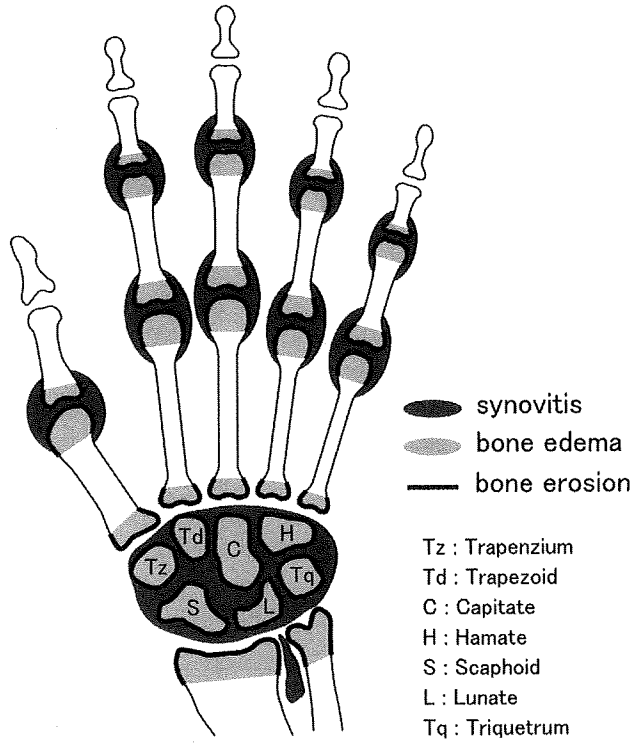

Fig. 1 Sites evaluated in calculating the compact magnetic resonance imaging (MRI) score. In this scoring system, 23 bones and 16 joints were evaluated. Pisiforme was excluded from the wrist bone evaluation. Bone erosion and edema were evaluated in 32 sites, and synovitis was evaluated in 11 sites. The score calculation is provided in detail in Table 2

examinations. All patients of both treatment groups (IFX and ETN) except one showed a moderate-to-good response, as assessed by DAS28–CRP, and none showed a recurrence of disease activity (Fig. 2).

Changes in cMRI score

Figure 2 and Table 3 provide details on the MRI scores calculated from the first and second imaging examinations for all patients. The first imaging identified seven patients with synovitis and three with bone edema in the finger joints. All patients showed bone erosion in the first and second imaging. However, erosion of the finger joints did not worsen in any of the patients included in this study, with ten of 13 patients showing an improvement over the intervening time period. Synovitis was present in the wrist joints of 12 patients at the first imaging, and although persistent, the second imaging showed improved synovitis in the wrist joints in most patients. Ten of the 13 patients showed bone edema in the wrist joint at the first imaging; by the second imaging, seven of these patients showed improvement, and three patients showed deterioration. Patient 1 of the IFX group showed remarkable joint destructions over the treatment time, while the others remained the same or showed a slight improvement.

Table 2 Compact MRI score (cMRIS) used in this study

Bone erosion	
Sites	Each wrist bone (except pisiforme), PIP (II–V), MCP (I–V), CM (I–V), carpal bones, distal radius and distal ulna, total of 23 bones, was scored separately.
Methods	Erosion was scored from 0 to 3, based on the proportion of the eroded bone relative to the assessed bone volume
	0: no erosion, 1: 1–33% of bone eroded, 2: 34–66% of bone eroded, 3: 67–100% of bone eroded.
	PIP and MCP joint was evaluated each proximal and distal side separately, and the score of the worse side was counted.
Bone edema	
Sites	Each wrist bone (except pisiforme), PIP (II–V), MCP (I–V), CM (I–V), carpal bones, distal radius and head of ulna was scored separately.
Methods	Bone edema was scored 0–3 according to the volume of edema relative to the assessed bone volume. The assessed bone volume in long bones was from the articular surface (or, if absent, its best estimated position) to a depth of 1 cm, while it was the whole bone in carpal bones
	0: no edema, 1: 1–33% of bone edematous, 2: 34–66% of bone edematous, 3: 67–100% of bone edematous.
	The PIP and MCP joints were evaluated on each proximal and distal side separately, and the score of the worse side was counted.
Synovitis	
Sites	Synovitis was assessed in 11 regions [PIP (II–V), MCP (I–V), the intercarpal and the distal radioulnar joint].
Methods	Synovitis was scored 0–3 according to the tertiles of the STIR high signal regions in the synovial compartment relative to the presumed maximum volume:
	0: normal (no synovitis), 1: mild, 2: moderate, 3: severe.
	The intercarpal joint score is doubled.
Proposed compact MRI score (cMRIS)	
cMRIS = (total bone erosion points) × 1.5 + (total bone edema points) × 1.25 + (total synovitis points) × 1	

PIP proximal interphalangea, *MCP* metacarpophalangea, *CM* carpo-metacarpa, *STIR* short tau inversion recovery

Relationship between cMRIS and DAS28-CRP

We evaluated the correlation between ΔcMRIS and ΔDAS28 in our small cohort and observed a positive correlation between the two scores ($R = 0.055$, $P < 0.05$; Fig. 3). However, one patient (IFX group patient 1) showed a very small change in the DAS28–CRP (2.66–2.83),

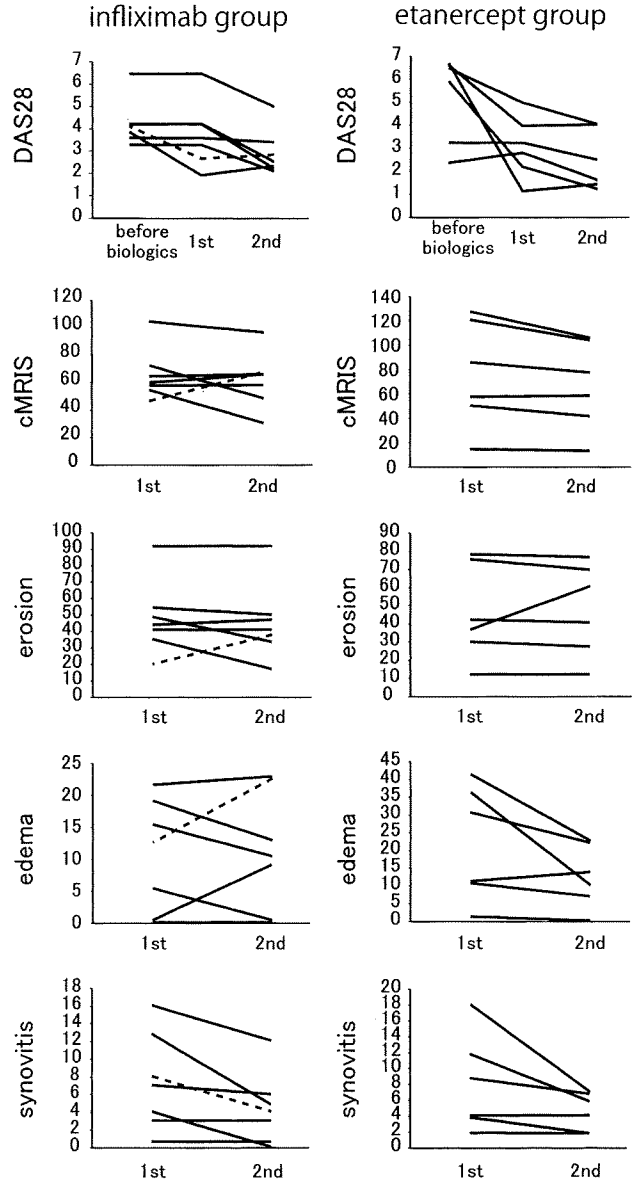

Fig. 2 Serial changes in disease activity score on 28 joints (*DAS28*) and compact MRI score (*cMRIS*) between first (*1st*) and second (*2nd*) MRI examinations. All patients except one had a good or moderate response to the biologics, and none showed increased disease activity. The cMRIS scores generally decreased or remained constant. However, one patient of the infliximab group showed an increase in cMRIS score even under low disease activity (*dotted line*)

indicating clinical remission but a marked worsening of the cMRIS (from 46.5 to 67.5).

Discussion

Rheumatoid arthritis is a chronic bone destruction disease that severely and progressively afflicts the patient's daily activities. Biologics, including TNF blockers, have recently

Table 3 Changes in compact MRI score during the present study

Patient	MRI scan	Finger joints			Wrist joints			Total cMRIS	DAS28	DAS28 at the introduction of biologics	Response
		Synovitis	Bone edema	Bone erosion	Synovitis	Bone edema	Bone erosion				
Infliximab group											
Patient 1	1st	0	0	6	7	12.5	21	46.5	1st 2.66	4.1	Good
	2nd	0	0	9	6	22.5	30	67.5	2nd 2.83		Good
	ΔcMRIS	0	0	3	−1	10	9	21	ΔDAS28 0.17		
Patient 2	1st	0	0	15	0	18.75	21	54.75	1st 4.22	4.19	No response
	2nd	0	0	9	0	12.5	9	30.5	2nd 2.51		Good
	ΔcMRIS	0	0	−6	0	−6.25	−12	−24.25	ΔDAS28 −1.71		
Patient 3	1st	1	1.25	18	2	20	22.5	64.75	1st 1.92	3.84	Good
	2nd	1	1.25	18	2	21.25	22.5	66	2nd 2.33		Good
	ΔcMRIS	0	0	0	0	1.25	0	1.25	ΔDAS28 0.41		
Patient 4	1st	6	0	6	7	0	85.5	104.5	1st 6.47	6.46	No response
	2nd	0	0	6	5	0	85.5	96.5	2nd 4.97		Moderate
	ΔcMRIS	−6	0	0	−2	0	0	−8	ΔDAS28 −1.5		

Table 3 continued

Patient	MRI scan	Finger joints			Wrist joints			Total cMRIS		DAS28	DAS28 at the introduction of biologics	Response
		Synovitis	Bone edema	Bone erosion	Synovitis	Bone edema	Bone erosion					
Patient 5	1st	0	0	4.5	4	0	49.5	58	1st	3.58	3.58	
	2nd	0	0	3	0	8.75	46.5	58.25	2nd	3.38		No response
	ΔcMRIS	0	0	−1.5	−4	8.75	−3	0.25	ΔDAS28	−0.2		
Patient 6	1st	3	0	3	13	5	42	66	1st	4.21	4.21	
	2nd	1	0	3	11	0	45	60	2nd	2.23		Good
	ΔcMRIS	−2	0	0	−2	−5	3	−6	ΔDAS28	−1.98		
Patient 7	1st	2	0	6	6	15	43.5	72.5	1st	3.27	3.27	
	2nd	0	0	6	4	10	28.5	48.5	2nd	2.09		Moderate
	ΔcMRIS	−2	0	0	−2	−5	−15	−24	ΔDAS28	−1.18		
Etanercept group												
Patient1	1st	2	0	16.5	7	11.25	13.5	50.25	1st	0.99	6.34	Good
	2nd	2	0	12	5	7.5	15	41.5	2nd	1.29		Good
	ΔcMRIS	0	0	−4.5	−2	−3.75	1.5	−8.75	ΔDAS28	0.3		
Patient 2	1st	0	0	1.5	12	36.25	36	85.75	1st	2.66	2.33	No response
	2nd	0	0	3	6	10	58.5	77.5	2nd	1.48		Moderate
	ΔcMRIS	0	0	1.5	−6	−26.25	22.5	−8.25	ΔDAS28	−1.18		
Patient 3	1st	1	1.25	7.5	1	0	4.5	15.25	1st	3.85	5.75	Moderate
	2nd	1	0	7.5	1	0	4.5	14	2nd	3.91		Moderate
	ΔcMRIS	0	−1.25	0	0	0	0	−1.25	ΔDAS28	0.06		
Patient 4	1st	0	0	6	4	41.25	70.5	121.75	1st	4.83	6.5	Moderate
	2nd	0	0	7.5	2	32.5	63	105	2nd	3.91		Moderate
	ΔcMRIS	0	0	1.5	−2	−8.75	−7.5	−16.75	ΔDAS28	−0.92		
Patient 5	1st	0	0	28.5	4	11.25	13.5	57.25	1st	2.05	6.55	Good
	2nd	0	0	28.5	4	13.75	12	58.25	2nd	1.08		Good
	ΔcMRIS	0	0	0	0	2.5	−1.5	1	ΔDAS28	−0.97		
Patient 6	1st	8	13.75	31.5	10	17.5	46.5	127.25	1st	3.09	3.09	
	2nd	3	11.25	30	4	11.25	46.5	106	2nd	2.35		Moderate
	ΔcMRIS	−5	−2.5	−1.5	−6	−6.25	0	−21.25	ΔDAS28	−0.74		

cMRIS Compact magnetic resonance imaging score, *DAS28* disease activity score in 28 joints, *CRP* C-reactive protein, *ΔcMRIS* changes in cMRIS value

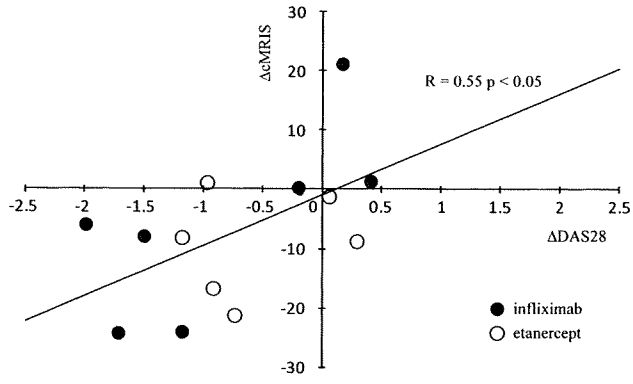

Fig. 3 Relationship between changes in the cMRIS value (ΔcMRIS) and changes in the DAS28 (ΔDAS28). ΔcMRIS and ΔDAS28 are the differences between the first and the second images. A positive correlation was observed between two evaluations ($R = 0.55$, $P < 0.05$)

raised the hope of RA sufferers of dramatic improvements in joint mobility and prognosis. The Trial of Etanercept and Methotrexate with Radiographic Patient Outcomes (TEMPO) study revealed the possibility of joint repair through treatment with ETN plus methotrexate [11]. However, many such studies used conventional radiography to evaluate bone erosion. Brown et al. [12] reported that about 96% patients treated with conventional disease-modifying antirheumatic drugs (DMARDs) achieved clinical remission according to the criteria of the American College of Rheumatology (ACR) and DAS28 score, but they still showed synovitis as assessed by MRI. The same percentage of asymptomatic patients with clinically normal joints also had synovitis based on MRI, while 46% showed bone marrow edema. In a comparative study on the therapeutic effectiveness of DMARDs and anti-TNF biologics, Martinez-Martinez et al. [13] also reported considerable synovitis based on MRI scans. This was still the case even in patients declared to be in clinical remission based on the biologics. These authors also reported no significant correlation between the improvement of clinical or laboratory data and MRI findings. Takes together, these studies stress the necessity of including an MRI examination in order to comprehensively evaluate total disease activity and joint damage in RA.

The imaging position and time needed for whole-body MRI makes it impractical for many rheumatologists to use and burdensome for the patient. Low-field extremity MRI is thus a valuable alternative that has recently become commercially available and has been tested for the diagnosis and monitoring of RA. Low-field extremity MRI improves patient comfort, is cost-effective for the institute, and yields equivalent results to whole-body MRI in terms of RA evaluation [14]. In support of this, using low-field extremity MRI, Savnik et al. [15] achieved a diagnostic accuracy for synovitis, bone edema, and bone erosion in RA comparable to that of high-field MRI.

Crues et al. [16] further reported that low-field dedicated-extremity MRI is more sensitive for detecting erosive changes in RA than radiography. In patients followed over 8 months, 30% demonstrated an increase in the size or number of erosions by MRI, while radiography revealed changes in only 0.8% of the patient cohort. Low-field dedicated-extremity MRI retains adequate imaging performance, but at a lower cost and with greater comfort and convenience for the patient. However, a limitation of low-field MRI is that the FOV is too small to enable an assessment of the hands and wrists in one examination. As wrist to PIP joints are usually affected in RA, examining the wrist to hand in one sequence is important for diagnosing and monitoring RA. Another disadvantage is that low-field MRI systems are not practical for small clinics to install because of their size and weight. To address these limitations and to render MRI more useful for RA diagnosis and treatment, we have developed a new low-field extremity MRI. This system has a large enough FOV to assess wrist to PIP joints in one examination, is lighter than its predecessor, and requires less total area to install.

The general adoption of MRI in general practice has also been hindered by a second problem. Many studies have used the RAMRIS OMERACT scoring method for MRI evaluation. However, this scoring method is too complex for use in daily medical examinations and treatments. We have used a new scoring system, cMRIS, for evaluating disease activity in RA patients treated with anti-TNF biologics. This method evaluates bone erosion, bone edema, and synovitis as well as RAMRIS. The RAMRIS scored bone erosion on a scale of 0–10 by its volume, which may be inconvenient. In addition, the RAMRIS method requires 2-D analysis. Therefore, we have improved this point and developed cMRIS. The cMRIS scores bone erosion on a scale of 0–3 by its volume, just as the method used for edema and synovitis. Considering the irreversibility of each finding, we decided that the coefficients for each finding should be 1.5 for bone erosion, 1.25 for bone edema, and 1 for synovitis. Based on the positive correlation that we obtained between ΔDAS28 and ΔcMRIS, we consider our scoring system to be useful in linking MRI image evaluation to clinical evaluation. However, a future large-scale study will be necessary to examine whether these coefficients are appropriate. Another problem is that synovitis cannot be evaluated precisely because we did not use gadolinium enhancement in our MRI system. As gadolinium enhancement requires intravenous injection and may induce severe side effects, such as nephrogenic systemic fibrosis, it cannot always be used in daily practice, especially in a small clinic. The problem of inaccuracy due to not using gadolinium can be

solved to some extent through the acquisition of experience. As the aim of our study was to establish the evaluation of RA disease activity by MRI in daily practice, we did not use gadolinium enhancement and instead developed an easier system to image and to facilitate the evaluations of these images.

In almost all patients, a positive correlation was observed between ΔDAS28 and ΔcMRIS. However, one patient in the IFX group showed a worsening of bone destruction when evaluated by cMRI even though the estimated DAS28–CRP indicated clinical remission. Prior to treatment, this patient had moderate disease activity (DAS28–CRP 4.1). She then responded well to the treatment and remained close to clinical remission during the study. The MRI scan showed a DAS28–CRP of 2.66 at the first imaging and 2.83 at the second imaging. However, both bone edema and erosion had worsened, as evidenced by the MRI scan. This patients provides good proof of how we can understand real disease activity using not only the DAS28 but also the cMRI in daily practice. In the future, rheumatologists should estimate real disease activity by MRI and other tools in addition to clinical activity as estimated by the DAS28.

Low-field extremity MRI has been reported to record a lower sensitivity than whole-body MRI in terms of bone edema assessment [17], and different sensitivities have been reported among different models [18]. We did not compare our cMRI image and the 1.5-T whole-body MRI image. However, work is now ongoing to develop an improved system, the 0.3-T MRI machine, called the compacTscan, which will enable a higher resolution and sensitivity imaging, and a more precise diagnosis of RA. To date, we have compared the 0.3-T cMRI image and the 1.5-T whole-body MRI image in three patients and obtained almost the same results (data not shown). The low-field extremity MRI is convenient for both patients and rheumatologists, and its use in daily practice could assist clinicians both in making an earlier diagnosis of RA and a more precise estimation of disease activity. The hope is that joint prognosis of RA patients will be improved using cMRI.

In conclusion, the results of our study have shown a positive correlation between ΔcMRIS and ΔDAS28, suggesting that cMRI and the cMRIS are useful for estimating total disease activity and joint damage in RA.

References

1. Cush JJ. Early rheumatoid arthritis—is there a window of opportunity? J Rheumatol Suppl. 2007;80:1–7.
2. Klarlund M, Ostergaard M, Jensen KE, Madsen JL, Skjødt H, Lorenzen I. Magnetic resonance imaging, radiography, and scintigraphy of the finger joints: one year follow up of patients with early arthritis The TIRA Group. Ann Rheum Dis. 2000;59:521–8.
3. McQueen FM, Stewart N, Crabbe J, Robinson E, Yeoman S, Tan PL, et al. Magnetic resonance imaging of the wrist in early rheumatoid arthritis reveals progression of erosions despite clinical improvement. Ann Rheum Dis. 1999;58:156–63.
4. Taylor PC. The value of sensitive imaging modalities in rheumatoid arthritis. Arthritis Res Ther. 2003;5:210–3.
5. Ostergaard M, Szkudlarek M. Imaging in rheumatoid arthritis—why MRI and ultrasonography can no longer be ignored. Scand J Rheumatol. 2003;32:63–73.
6. Haavardsholm EA, Bøyesen P, Østergaard M, Schildvold A, Kvien TK. Magnetic resonance imaging findings in 84 patients with early rheumatoid arthritis: bone marrow edema predicts erosive progression. Ann Rheum Dis. 2008;67:794–800.
7. Taouli B, Zaim S, Peterfy CG, Lynch JA, Stork A, Guermazi A, et al. Rheumatoid arthritis of the hand and wrist: comparison of three imaging techniques. AJR Am J Roentgenol 2004;182:937–43.
8. Savnik A, Malmskov H, Thomsen HS, Bretlau T, Graff LB, Nielsen H, et al. MRI of the arthritic small joints: comparison of extremity MRI (0.2 T) vs high-field MRI (1.5 T). Eur Radiol. 2001;11:1030–8.
9. Østergaard M, Peterfy C, Conaghan P, McQueen F, Bird P, Ejbjerg B, et al. OMERACT Rheumatoid Arthritis Magnetic Resonance Imaging Studies Core set of MRI acquisitions, joint pathology definitions, and the OMERACT RA-MRI scoring system. J Rheumatol. 2003;30:1385–6.
10. McQueen F, Lassere M, Edmonds J, Conaghan P, Peterfy C, Bird P, et al. OMERACT Rheumatoid Arthritis Magnetic Resonance Imaging Studies. Summary of OMERACT 6 MR Imaging Module. J Rheumatol. 2003;30:1387–92.
11. Klareskog L, van der Heijde D, Jager JP, Gough A, Kalden J, Malaise M, et al. Therapeutic effect of the combination of etanercept and methotrexate compared with each treatment alone in patients with rheumatoid arthritis: double-blinded randomized controlled trial. Lancet. 2004;363:675–81.
12. Brown AK, Quinn MA, Karim Z, Conaghan PG, Peterfy CG, Hensor E, et al. Presence of significant synovitis in rheumatoid arthritis patients with disease-modifying antirheumatic drug-induced clinical remission: evidence from an imaging study may explain structural progression. Arthritis Rheum. 2006;54:3761–73.
13. Martinez-Martinez MU, Cuevas-Orta E, Reyes-Vaca G, Baranda L, Gonzalez-Amaro R, Abud-Mendoza C. Magnetic resonance imaging in patients with rheumatoid arthritis with complete remission treated with disease-modifying antirheumatic drugs or anti-tumour necrosis factor alpha agents. Ann Rheum Dis. 2007;66:134–5.
14. Taouli B, Zaim S, Peterfy CG, Lynch JA, Stork A, Guermazi A, et al. Rheumatoid arthritis of the hand and wrist: comparison of three imaging techniques. AJR Am J Roentgenol.. 2004;182:937–43.
15. Savnik A, Malmskov H, Thomsen HS, Bretlau T, Graff LB, Nielsen H, et al. MRI of the arthritic small joints: comparison of extremity MRI (0.2 T) vs high-field MRI (1.5 T). Eur Radiol. 2001;11:1030–8.
16. Crues JV, Shellock FG, Dardashti S, James TW, Troum OM. Identification of wrist and metacarpophalangeal joint erosions using a portable magnetic resonance imaging system compared to conventional radiographs. J Rheumatol. 2004;31:676–85.
17. Bird P, Ejbjerg B, Lassere M, Østergaard M, McQueen F, Peterfy C, et al. A multireader reliability study comparing conventional high-field magnetic resonance imaging with extremity low-field MRI in rheumatoid arthritis. J Rheumatol. 2007;34:854–6.
18. Duer-Jensen A, Ejbjerg B, Albrecht-Beste E, Vestergaard A, Møller Døhn U, Lund Hetland M, et al. Does low-field dedicated extremity MRI (E-MRI) reliably detect RA bone erosions? A comparison of two different E-MRI units and conventional radiography with high resolution CT. Ann Rheum Dis. 2008. doi: 10.1136/ard.2008.093591.

Mod Rheumatol (2009) 19:366–371
DOI 10.1007/s10165-009-0174-0

ORIGINAL ARTICLE

Altered peptide ligands regulate type II collagen-induced arthritis in mice

Ei Wakamatsu · Isao Matsumoto · Yohei Yoshiga · Taichi Hayashi · Daisuke Goto · Satoshi Ito · Takayuki Sumida

Received: 4 March 2009 / Accepted: 2 April 2009 / Published online: 12 May 2009

Abstract We reported that peripheral blood mononuclear cells from HLA-DRB1*0101 Japanese patients with rheumatoid arthritis (RA) were highly reactive to 256–271 peptide of type II collagen (CII). Similar to RA, T cells reactive to CII (AA256–271) play a crucial role in the generation of arthritis in CII-induced arthritis mouse ($I\text{-}A^q$). In the present study, we regulated the CII reactivity of T cells from CIA mouse with $I\text{-}A^q$ by altered peptide ligand (APL). Eight different APLs were designed and screened for their antagonistic activity using CII reactive cytokine production assay. Four APLs of CII 256–271 exhibited antagonistic activity in CII-reactive T cells. Moreover, intraperitoneally injected APL-5 (G262A) significantly suppressed CII-induced arthritis in mice, whereas the other three APLs did not. Compared with the control, APL-5 suppressed interleukin (IL)-17 production by T cells from CII-induced arthritis mice. These results suggest that CII APL is a potentially suitable therapeutic strategy for the control of RA.

Keywords Altered peptide ligand · Antagonist · Type II collagen-induced arthritis · T cells

E. Wakamatsu is a research fellow of the Japan Society for the Promotion of Science.

E. Wakamatsu · I. Matsumoto · Y. Yoshiga · T. Hayashi · D. Goto · S. Ito · T. Sumida (✉)
Division of Clinical Immunology,
Doctoral Programs in Medical Sciences,
Major of Advanced Biomedical Applications,
Graduate School Comprehensive Human Science,
University of Tsukuba, 1-1-1 Tenodai,
Tsukuba, Ibaraki 305-8575, Japan
e-mail: tsumida@md.tsukuba.ac.jp

Introduction

Rheumatoid arthritis (RA) is an autoimmune disease characterized by persistent inflammatory synovitis leading to various degrees of cartilage destruction, bone erosion, and ultimately joint deformity and loss of joint function. Although the pathogenesis of RA is not clear, there is sufficient evidence to suggest the involvement of T cells in the inflammatory process, such as the infiltration of T cells, especially $CD4^+$ $CD45RO^+$ T cells, in joints of RA patients [1]. Furthermore, the susceptibility to RA is associated with HLA-DRB1 genes [2].

Type II collagen (CII), a molecule abundant in the articular cartilage, is considered one of the target autoantigens in RA. CII-reactive T cell clones have been established in vitro from synovial T cells of RA [3]. Sekine et al. [4] suggested that the expansion of oligoclonal T cells in RA joints is driven by stimulation of CII. Furthermore, the pathology in CII-induced arthritis (CIA) mice is similar to that in RA synovium. The susceptibility to CIA is determined by $I\text{-}A^q$, which is a major histocompatibility complex (MHC) class II molecule, and the immunodominant CII256–271 region of CII could be bound to $I\text{-}A^q$ molecules [5].

T cell activation depends on the ability of the T cell receptor (TCR) to recognize 8–20 amino acid peptides that are bound to MHC molecules. The process of recognition of peptides by TCR is flexible. If the amino acid residue of peptide ligands for TCR is substituted for a different amino acid and can still bind to the MHC molecules (altered peptide ligands, APLs), these APLs could regulate the activation of T cells. Several studies [6, 7] have shown that APL can potentially induce differential cytokine secretion, anergy, and antagonism of the response to wild-type antigens. Therefore, it is possible to use APL as a therapeutic

agent against T-cell-mediated diseases such as autoimmune diseases.

Our previous report [8] demonstrated that peripheral blood mononuclear cells from HLA-DRB1*0101 Japanese patients with RA were highly reactive to the 256–271 peptide of CII, and designed APLs suppressed T cell response to the immunodominant epitope (CII256–271) of CII. In the present study, we tried to regulate the CII-reactive T cells from CIA by eight different APLs to CII256–271. The results showed that four APLs could suppress the CII-reactive immune response in vitro and one APL exhibited an inhibitory effect on arthritis in vivo. These results suggest that the application of CII APL is a potentially suitable therapeutic strategy in the control of RA.

Materials and methods

Mice

DBA/1 J mice were purchased from The Charles River Laboratory (Yokohama, Japan). They were maintained in specific pathogen-free conditions in the laboratory animal resource center. All experiments were performed according to the *Guide for the Care and Use of Laboratory Animals* at Tsukuba University.

Induction of arthritis

Mice were immunized intradermally with 100 μg bovine type II collagen (CII: Collagen Research Center, Tokyo, Japan) in Complete Freund's adjuvant (CFA; Difco, Detroit, MI, USA). Each mouse received a booster dose on day 21 by intraperitoneal injection of 100 μg CII.

CII (256–271) peptide and altered peptide ligands

The peptide representing CII (AA256–271) and its altered peptide ligands (APL) containing specific amino acid substitutions were chemically synthesized by solid-phase procedure and purified by high-performance liquid chromatography (OPERON Biotechnologies, Tokyo).

Pre-pulse assay

Mice were immunized with 100 μg CII emulsified with CFA. Twelve days after immunization, the mice were anesthetized and the spleens removed. The spleen was treated with collagenase D (Roche, Mannheim, Germany), and $CD11c^+$ cells were isolated by CD11c microbeads (Miltenyi Biotec, Tokyo). The cells were pulsed with 50 μM CII256–271 peptides for 2 h. After washing, they were adjusted to 1×10^6 cells/ml and pulsed with 200 μM APLs for 12 h. On the other hand, $CD4^+$ cells were isolated using CD4 microbeads (Miltenyi Biotec) from splenocytes of mice immunized with CII. Then they were adjusted to 5×10^5 cells/ml and added to the plate where $CD11c^+$ cells were cultured for 12 h. The supernatants were collected 72 h later and interferon-γ (IFN-γ), IL-17, IL-2, IL-4, and IL-10 were measured by enzyme-linked immunosorbent assay (ELISA) (IL-17 and IL-2; BioLegend, San Diego, CA, IFN-γ, IL-4 and IL-10; eBioscience, San Diego, CA).

Treatment with APLs

Mice were treated with three injections each of 333 μg of APLs intraperitoneally (total 1 mg) on days 24, 26, and 28 after the first immunization with CII. The animals were observed at 3-day intervals and evaluated for the severity of arthritis by scoring each paw. The score ranged from 0 to 3 (0, no swelling or redness; 1, swelling or redness in one joint; 2, involvement of two or more joints; 3, severe arthritis of the entire paw and joints). The score of each animal was the sum of scores for all four paws.

Histopathology

The ankles were removed on day 60 after the first immunization with CII and fixed in 3% buffered formalin. The paws were decalcified in ethylenediaminetetraacetic acid (EDTA) in buffered formalin, embedded in paraffin, sectioned, and stained with hematoxylin and eosin.

Analysis of T cell response

Mice were treated with APLs by the above method. Their splenocytes were removed on day 35 after immunization, and $CD4^+$ cells and $CD11c^+$ cells were isolated by microbeads as described above. $CD4^+$ cells and $CD11c^+$ cells (5:1) were mixed and cultured with denatured CII (10 μg/ml), and supernatants were collected 24 h later. The amounts of IL-17 and IFN-γ were measured by ELISA.

Statistical analysis

The Mann–Whitney *U* test was used for statistical analysis. *P* values less than 0.05 denoted significant difference.

Results

Antagonistic activity of APLs in vitro

We designed eight different APLs as shown in Fig. 1a. We screened these APLs for their antagonistic activity

(A)

					P1	P2	P3	P4	P5	P6	P7	P8				
CII256-271	G	K	P	G	I	A	G	F	K	G	E	Q	G	P	K	G
APL-1	-	-	-	-	-	S	-	-	-	-	-	-	-	-	-	-
APL-2					-	D	-	-	-	-	-	-	-	-	-	-
APL-3	-	-	-	-	-	-	D	-	-	-	-	-	-	-	-	-
APL-4	-	-	-	-	-	-	K	-	-	-	-	-	-	-	-	-
APL-5	-	-	-	-	-	-	A	-	-	-	-	-	-	-	-	-
APL-6	-	-	-	-	-	-	-	-	A	-	-	-	-	-	-	-
APL-7	-	-	-	-	-	-	-	-	V	-	-	-	-	-	-	-
APL-8	-	-	-	-	-	-	-	-	M	-	-	-	-	-	-	-

(B)

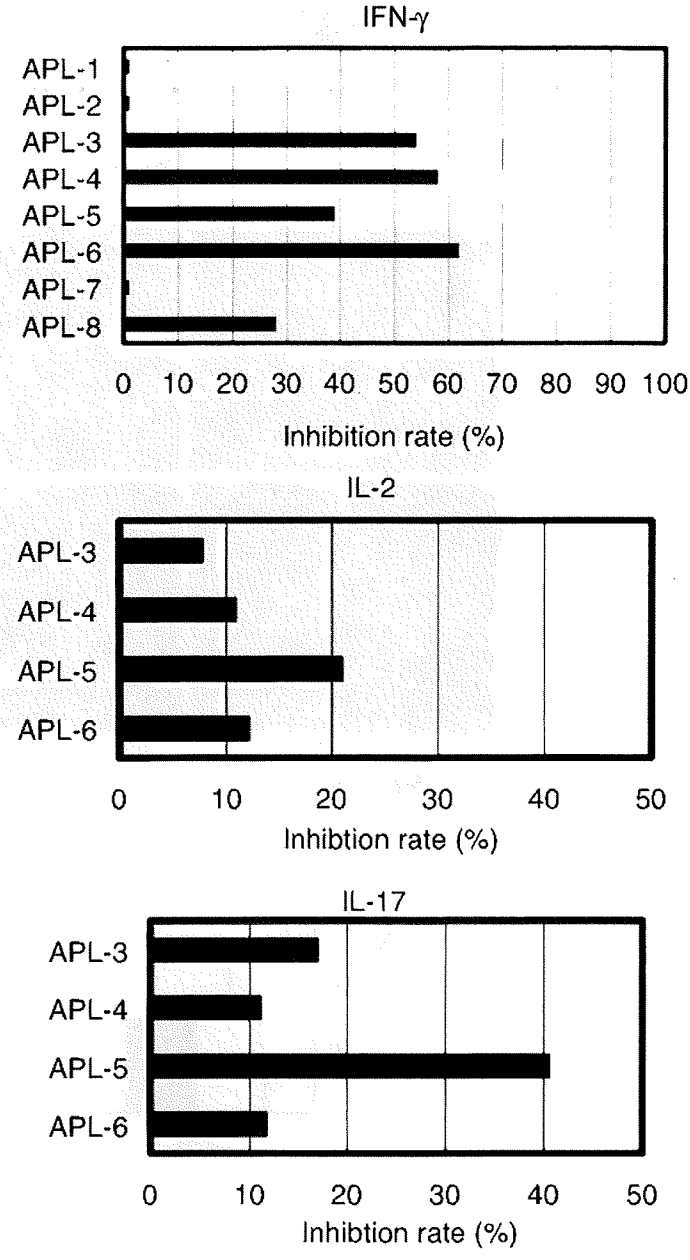

Fig. 1 Screening of APLs with antagonistic activity. **a** Altered peptide ligands were designed based on the I-A^q anchor motif. P1, P4, and P7 were predicted anchor position in CII256–271 peptide. **b** DBA/1 mice were immunized with CII. Antagonistic activity of APLs was investigated using CD4 T cells on day 12 after immunization by pre-pulse assay described in "Materials and Methods." Concentrations of IFN-γ, IL-2, and IL-17 were measured in the culture supernatants by ELISA. Inhibition rates of IFN-γ, IL-2 and IL-17 are expressed as percentage inhibition against the CII 256–271 peptide response. Data are representative of three similar experiments ($n = 3$)

using CII-reactive cytokine production assay. Four APLs (APL-3, -4, -5, and -6) suppressed (by more than 30–60%) production of CII256–271-reactive IFN-γ in vitro (Fig. 1b). We also investigated whether APL-3, -4, -5, and -6 suppressed the production of other cytokines. Similar to IFN-γ, the four APLs suppressed production of IL-2 and IL-17

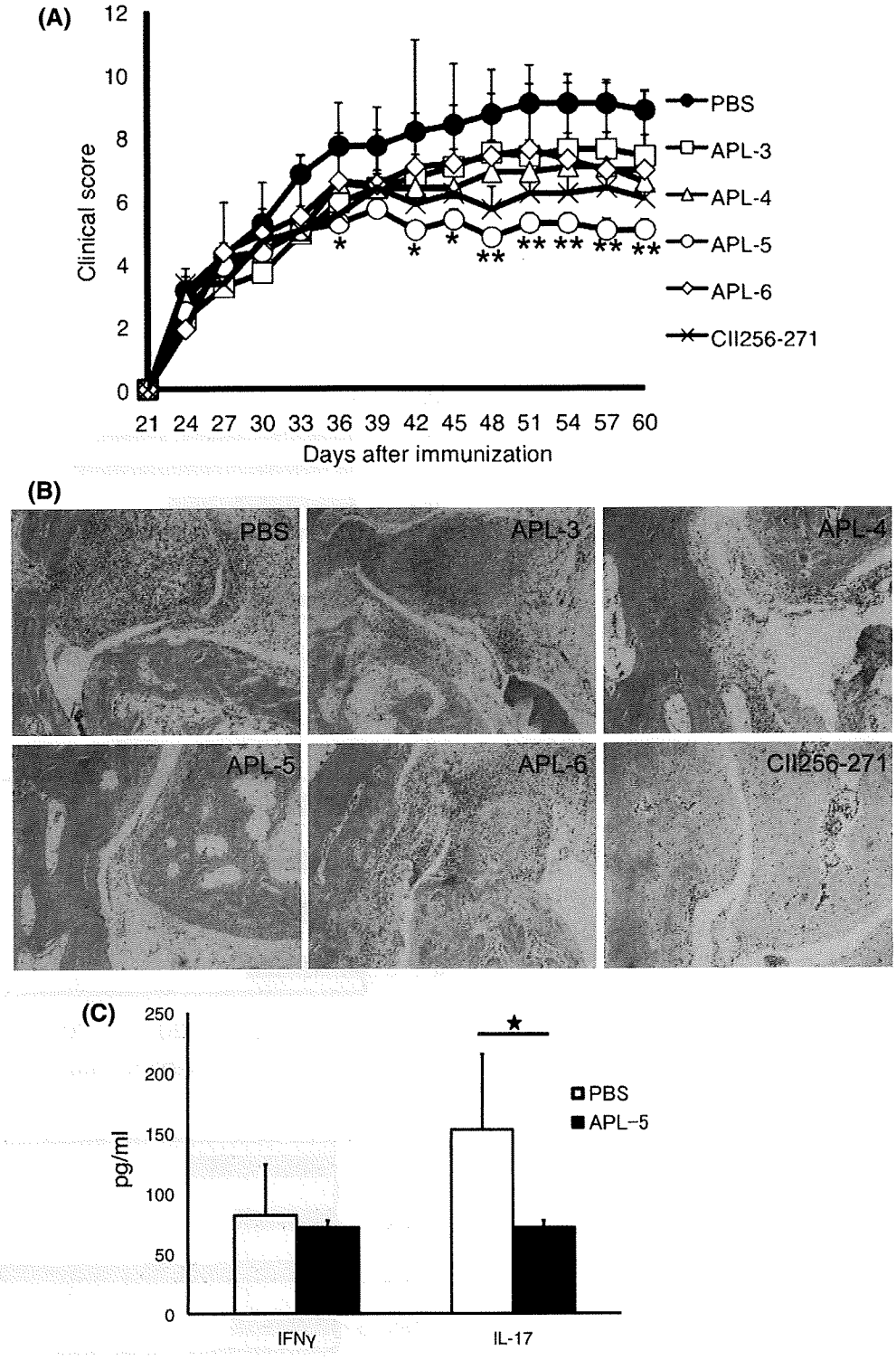

Fig. 2 Therapeutic effect of G262A in CIA. **a** DBA/1 mice were immunized and boosted with CII. Four APLs, CII256–271 peptide, and PBS were administered i.p. on days 24, 26, and 28 after immunization of CII (each $n = 9$), respectively. The clinical score of arthritis is expressed as mean ± standard error of the mean (SEM). $^{*}P < 0.01$, $^{**}P < 0.001$ versus PBS. **b** Each mouse was sacrificed on day 60 after immunization, and the ankles were examined by H&E staining. **c** On day 7 after the administration of APLs, $CD4^{+}$ T cells and dendritic cells were isolated from the spleen and co-cultured for 24 h. IFN-γ and IL-17 concentrations were measured by ELISA. T cell response of mice injected with PBS was assigned as 1. Data are mean ± standard deviation (SD) with triplicate culture. $^{*}P < 0.05$ versus PBS

(Fig. 1b). However, IL-4 and IL-10 were not detected in any samples (data not shown). Thus, we considered these four APLs as candidates for antagonistic APLs and used them in further experiments in vivo.

APL-5 results in significant suppression of arthritis

To investigate the therapeutic effects of the above four APLs on arthritis in vivo, we treated CII mice immunized

with APL intraperitoneally on day 24. CII256–271 peptide and phosphate-buffered saline (PBS) were injected as negative control. The results showed that APL-5 significantly suppressed the development of arthritis compared with the other three APLs ($P < 0.01$) and PBS ($P < 0.001$) (Fig. 2a). These mice were sacrificed on day 60 after immunization of CII, and histological examination was performed. As shown in Fig. 2b, APL-5 inhibited mononuclear cell infiltration compared with the other three APLs and PBS. These results indicate that CII-induced arthritis could be regulated by APL-5. T cell predominant epitope by itself (CII256–271) slightly decreased the severity of arthritis, suggesting activation-induced cell death by the excess dose of dominant epitope.

Effects of APLs on cytokine production

To examine whether APLs suppress CII-reactive T cells in vivo, we investigated the production of IFN-γ and IL-17 from CII-reactive T cells in APLs-treated mice. As shown in Fig. 2c, injection of APL-5 significantly suppressed IL-17 production, but not that of IFN-γ, by CII-reactive T cells ($P < 0.05$). The other APLs and CII256–271 peptides did not have any effects on the production of IFN-γ and IL-17 (data not shown).

Discussion

Several investigators [9–11] demonstrated the protective effects of APL using experimental autoimmune encephalomyelitis (EAE) and CIA. Co-immunization of mice bearing the H-2^u haplotype with an APL and an encephalogenic peptide prevented the development of EAE [9]. Furthermore, Myers et al. [10] showed that APL regulated the onset of CIA in H-2^q mice. Although their reports showed the protective activity of APL, the therapeutic effects of APLs have been hardly reported. Myers et al. [12] reported that administration of their APLs on day 28 after CII immunization decreased the incidence rate of arthritis though they did not show the score of arthritis of those mice. Zhao et al. [13] demonstrated that collagen-induced arthritis in rat was suppressed by oral administration of APLs after the onset of arthritis. These observations support the notion that their APLs might be a therapeutic strategy against arthritis. In the present study, administration of APL-5 after the onset of arthritis suppressed the development of CIA, indicating the therapeutic effect of APL on CIA. In contrast, Myers's study [12] administered APLs to CIA mice at the onset of arthritis. The experiments by Zhao et al. [13] were designed with oral administration and done using rat model. The most important message from this study is that APL-5 is common between CIA mice and patients with RA [8], indicating that clinical trial can be hoped for in the near future.

Several studies have examined the role of Th17 cells in CIA. Development of CIA was regulated in IL-17 knockout mice, suggesting that IL-17 plays a crucial role in arthritis [14]. Severe clinical and histologic CIA was induced in IFN-γ receptor knockout mice [15], whereas CIA was suppressed by the administration of anti-IFN-γ antibodies [16]. Therefore, the role of IFN-γ in the development of CIA is controversial. Our studies showed that APL-5 inhibited CII-reactive IL-17 production in vivo, suggesting the main contribution of IL-17 on the development of CIA.

Our experiments in vivo showed the possibility that each APL had different effect on T cell subset. APL-5 preferentially suppressed IL-17 but not IFN-γ; on the other hand, APL-6 suppressed IFN-γ but not IL-17. Although the precise mechanism is not clarified, these findings suggest that minor variations of the peptide may affect the peptide-binding affinity, or minor change of the physicochemical properties of amino acid residues may involve TCR binding activity.

In conclusion, the present study showed that administration of APL-5 suppressed the development of CIA in mice. CII APL is a potentially suitable therapeutic strategy for the control of RA.

Acknowledgment This work was supported in part by a Research Grant from the Ministry of Health, Labor, and Welfare, and the Research Grant from the Ministry of Education, Culture, Sports, Science, and Technology.

Conflict of interest statement All of the authors confirm that they have no conflicts of interest with regard to this work.

References

1. Struyk L, Hawes GE, Dolhain RJ, van Scherpenzeel A, Godthelp B, Breedveld FC, et al. Evidence for selective in vivo expansion of synovial tissue-infiltrating CD4+CD45RO+T lymphocyte on the basis of CDR3 diversity. Int Immunol. 1994;6:897–907.
2. Fugger L, Svejgaard A. Association of MHC and rheumatoid arthritis. HLA-DR4 and rheumatoid arthritis: studies in mice and human. Arthritis Res Ther. 2000;2:208–11.
3. Londei M, Savill CM, Verhoef A, Brennan F, Leech ZA, Duance V, et al. Persistence of collagen type II-specific T cell clones in the synovial membrane of a patient with rheumatoid arthritis. Proc Natl Acad Sci USA. 1989;86:636–40.
4. Saeki T, Kato T, Masuko-Hongo K, Nakamura H, Yoshino S, Nishioka K, et al. Type II collagen is a target antigen of clonally expanded T cells in the synovium of patients with rheumatoid arthritis. Ann Rheum Dis. 1999;58:446–50.
5. Luross JA, Williams NA. The genetic and immunopathological processes underlying collagen-induced arthritis. Immunology. 2001;103:407–16.
6. Magistris MTD, Alexander J, Coggeshall M, Altman A, Gaeta FC, Grey HM, et al. Antigen analog-major histocompatibility